

Designing Chitosan–Dextran Sulfate Nanoparticles Using Charge Ratios

Received: November 16, 2006; Final Revision Received: June 6, 2007; Accepted: June 10, 2007; Published: November 30, 2007

Yan Chen,¹ Vellore J. Mohanraj,¹ Fang Wang,¹ and Heather A.E. Benson¹

¹School of Pharmacy, Curtin University of Technology, GPO Box U1987, Perth, Western Australia 6845

ABSTRACT

The purpose of this study was to examine the effect of charge ratio on the formation and properties of the chitosan (CS)–dextran sulfate (DS) nanoparticles developed for the delivery of water-soluble small and large molecules, including proteins. Rhodamine 6G (R6G) and bovine serum albumin (BSA) were chosen as model molecules. CS-DS nanoparticles were formulated by a complex coacervation process under mild conditions. The influence of formulation and process variables, including the charge ratio of the 2 ionic polymers, on particle size, zeta potential, and nanoparticle entrapment of R6G and BSA was studied. The *in vitro* release of R6G and BSA was also evaluated, and the integrity of BSA in the release fraction was assessed using sodium dodecyl sulfate–polyacrylamide gel electrophoresis. Depending on the concentration and charge ratio of DS and CS, nanoparticles with varied size (≥ 244 nm) and zeta potential (-47.1 – 60 mV) were obtained. High entrapment efficiency (98%) was achieved for both R6G and BSA when the charge ratio of the 2 ionic polymers was greater than 1.12. The release of both R6G and BSA from nanoparticles was based on the ion-exchange mechanism. BSA showed much slower continuous release for up to 7 days while still maintaining its integrity for an extended period. The CS-DS nanoparticles developed based on the modulation of charge ratio show promise as a system for controlled delivery of both small and large molecules, including proteins.

KEYWORDS: Chitosan, dextran sulfate, nanoparticles, charge ratio, protein delivery, sustained release.

INTRODUCTION

Chitosan (CS) has received a great deal of attention as a material of choice for the preparation of micro- and nanoparticles for parenteral, nasal, ophthalmic, transdermal, and implantable delivery of drugs, proteins, peptides, and gene materials.¹ This wide application of and strong interest in CS is derived from its unique structure and physicochemical properties.

CS, a natural linear polyamine with a high ratio of glucosamine to acetyl-glucosamine units, is a weak base and carries a positive charge. Its solubility is pH-dependent, and it reacts readily with negatively charged surfaces (via mucoadhesion) and materials, including polymers and DNA. These features and its biodegradability, low toxicity, and good biocompatibility make it versatile and attractive for use in biomedical and pharmaceutical formulations.^{2,3}

Ionic gelation, complex coacervation, emulsion cross-linking, and spray-drying are methods commonly used for the preparation of CS nanoparticles.^{1,4} Among those methods, ionic gelation (also known as ionotropic gelation) and complex coacervation are mild processes occurring in a pure aqueous environment and are ideal for maintaining the in-process stability of proteins and peptides. Ionic gelation and complex coacervation are very similar except that the former involves the gelation of CS using an electrolyte such as triphosphate (TPP),⁵ whereas the latter employs an oppositely charged ionic polymer such as alginate.⁶ Most researchers adapt the ionic gelation method developed by Calvo et al⁵ using CS and TPP for the incorporation of proteins.^{7,8} A new type of CS nanoparticle using dextran sulfate (DS) as a polyanionic polymer was developed to achieve complex coacervation for the incorporation and controlled release of an antiangiogenesis hexapeptide⁹; this was the first report describing the use of DS to formulate CS-based nanoparticles. The advantages of CS-DS nanoparticles are enhanced stability and increased mechanical strength compared with CS-TPP microparticles, whose lower stability and mechanical strength limit their usage in drug delivery.¹ Pan et al reported that CS-TPP nanoparticles could be dissolved in low-pH HCl in several minutes,¹⁰ whereas CS-DS nanoparticles were stable in low pH.¹¹ It has also been reported that DNA and insulin structures are protected when DS is used in the formulation of polyethylenimine (PEI)-DS nanoparticles.^{12,13} DS was also found capable of reducing the cationic charge-related cytotoxicity of PEI nanoparticles *in vitro*.¹² Therefore, it is possible that the combination of CS and DS as matrix materials, in an optimal charge ratio, may act synergistically to incorporate and protect proteins and drugs and may reduce the cytotoxicity of CS caused by its cationic charge.

Although there have been investigations of how the properties of CS and formulation variables such as CS molecular weight (MW), concentrations of CS and protein, and formulation pH affect the formation and encapsulation capability of nanoparticles,^{5,8,14} to our knowledge, no attempts

Corresponding Author: Yan Chen, School of Pharmacy, Curtin University of Technology, GPO Box U1987, Perth, Western Australia 6845. Tel: 61 8 9266 2738; Fax: 61 8 9266 2769; E-mail: y.chen@curtin.edu.au

have been made to study how the charge ratio of CS to the oppositely charged polymer influences the formulation and properties of nanoparticles. To test the hypothesis that the charge ratio of the 2 ionic polymers is critical for the formation of nanoparticles as well as the entrapment of ionic protein and drug molecules, this study focused on (1) the optimization of CS-DS nanoparticle formulation by examining how the concentration and charge ratio of CS:DS affected the formation of nanoparticles; (2) the effects of the weight and charge ratio of the 2 polymers on the protein and drug entrapment and their release; and (3) the use of charge ratio to estimate the level of entrapment of a small positively charged molecule, rhodamine 6G (R6G). In this study, bovine serum albumin (BSA) was chosen as a model protein and R6G as a water-soluble model drug.

MATERIALS AND METHODS

Materials

The polymer CS (medium MW 400 000 Da, 85% deacetylation) was purchased from Fluka/Sigma-Aldrich (Castle Hill, NSW, Australia). BSA (Fraction V, MW 66 000 Da), sodium phosphate dibasic (MW 141.96 Da), and R6G (MW 479 Da) were obtained from Sigma-Aldrich (Gillingham, Dorset, UK). Bradford reagent (Fraction Code no B-6916), Coomassie blue, sodium salt of DS (MW 12 750 Da), and Bradford protein assay kit were purchased from Sigma Chemical Co (St Louis, MO). Tris-glycine gradient gel was supplied by Gradipore Ltd (Frenchs Forest, NSW, Australia). Molecular standards used in sodium dodecyl sulfate-polyacrylamide gel electrophoresis (SDS-PAGE) were obtained from Bio-Rad Laboratories (Gladesville, NSW, Australia). All other solvents and materials were of analytical grade. Deionized water (Milli-Q water) was used in the preparation of buffers and standard solutions of protein. All other chemicals and reagents used in this study were of analytical grade.

Methods

Preparation of CS-DS Nanoparticles

CS-DS nanoparticles were prepared by the complex coacervation of CS and DS as described in a previous publication.⁹ To study the effects of the varying concentrations of CS and DS on the formation of nanoparticles, CS and DS solutions of 0.1%, 0.25%, 0.5%, and 1% (wt/vol) were prepared by dissolving various amounts of CS in aqueous acetic acid or DS in water. The concentration of acetic acid was kept 1.75 times higher than that of CS in all cases to maintain the CS in the solution. Variable volumes of DS solution (1, 2, 3, 4, 5, 5.8, and 10 mL) were then mixed with 5 mL of respective concentrations of the CS solution under magnetic stirring (~200 rpm) at room temperature. The nanoparticle/microparticle suspension was formed spon-

aneously. The mixture was stirred for a further 15 minutes. Both the pH and the particle size of the nanoparticle suspension were measured. All samples were then classified according to their size as 100 to 500 nm, 501 to 1000 nm, or >1000 nm, correlating to the formation of nanoparticles and microparticles.

Incorporation of BSA into nanoparticles was performed by dissolving BSA in either polycationic CS solution or polyanionic DS solution to obtain a BSA concentration of 1 mg/mL in the polymer. The BSA-loaded nanoparticles were formed spontaneously upon addition of a variable volume of 3 mL, 5 mL, and 8.5 mL (0.1% wt/vol) of the DS aqueous solution to 5 mL of the CS acidic solution (0.1% wt/vol) under magnetic stirring for 15 minutes.

Incorporation of R6G into CS-DS nanoparticles was performed by the addition of 16, 16, 32, and 16 mL of 0.9 mg/mL of R6G solution to 4 mL of 0.5%, 10 mL of 0.26%, 2 mL of 1.6%, and 16 mL of 0.2% (wt/vol) DS solution, respectively, before mixing with 20, 13, 8, and 8 mL of 0.1% (wt/vol) CS solution, respectively, to study the influence of the charge ratio on nanoparticle formulation.

Two stirring methods, magnetic stirring (approximately 200 rpm) and homogenization (approximately 1000 rpm), were applied to investigate the effect of stirring method on particle size.

Nanoparticle Morphology

The morphology of nanoparticles was characterized using both field emission scanning electron microscopy (FESEM) and transmission electron microscopy (TEM). For FESEM, nanoparticle powder was placed on metallic studs with double-sided carbon tape and coated with platinum by a sputter coater (JFC-1300, Auto Fine Coater, Jeol, Tokyo, Japan) for 40 seconds in a vacuum at a current intensity of 40 mA. The morphology of the particles was observed using a Leo Supra 55 Variable Pressure field emission scanning electron microscope (Oberkochen, Germany). For TEM characterization, samples were prepared by dispersing dried nanoparticle powder in distilled water. A drop of sample solution was placed on top of the copper grids and allowed to air dry, then coated with carbon. TEM pictures were taken with a CM 12 Philips transmission electron microscope (Philips, Amsterdam, Netherlands).

Particle Size and Zeta Potential

Nanoparticle size and size distribution were determined by photon correlation spectroscopy using a Zetasizer 3000HS (Malvern Instruments, Malvern, Worcestershire, UK). The measurements were performed at 25°C with a detection angle of 90°, and the raw data were subsequently correlated to Z average mean size using a cumulative analysis by the

Zetasizer 3000HS software package. Each sample was measured 10 times. The zeta potential of particles was determined by laser Doppler anemometry using a Zetasizer 3000HS. All analyses were performed on samples appropriately diluted with filtered deionized water. For each sample, the mean \pm SD of 3 repeat measurements was established.

Loading and Entrapment Efficiency of BSA and R6G

The amount of BSA or R6G entrapped in the nanoparticles was calculated by the difference between the total amount of protein added to the nanoparticle formation medium and the amount of nonentrapped protein remaining in the aqueous supernatants. The latter was determined following the separation of protein-loaded nanoparticles from the aqueous medium by centrifugation at 15 000 rpm and 4°C for 15 minutes. The supernatant was collected and the particles were washed with water and then subjected to another cycle of centrifugation. The amount of free BSA in the supernatants was determined by the Bradford protein assay.¹⁵ The unloaded R6G in supernatants was measured by UV-Vis spectrophotometry (UV 01201, Shimadzu Corporation, Kyoto, Japan) and a fluorometer (Cary Eclipse, Varian Instruments, Mulgrave, Victoria, Australia). The BSA and R6G loading and entrapment efficiency were calculated from the following equations:

$$\text{Loading (\%)} = \left(\frac{\text{Amount M Added} - \text{Amount of Free M}}{\text{Weight of Nanoparticles}} \right) \times 100 \quad (1)$$

$$\text{Entrapment Efficiency (\%)} = \left(\frac{\text{Amount M Added} - \text{Amount of Free M}}{\text{Amount M Added}} \right) \times 100 \quad (2)$$

where M represents BSA or R6G.

Analysis of BSA by Bradford Protein Assay

The BSA-containing samples (0.1 mL), prepared in triplicate, were mixed with 3 mL of Bradford reagent at room temperature. The absorbance of samples at 595 nm was measured after 2 minutes and before 1 hour of the reaction in a 3-mL cuvette against a reagent blank prepared from 0.1 mL of water and 3 mL of Bradford reagent. The concentration of BSA in samples was determined from a BSA standard calibration curve obtained by the same procedure.

Analysis of R6G

The concentration of R6G was measured first by UV-Vis spectrophotometry at 524 nm. Then the samples were diluted at appropriate times and accurately analyzed by the

fluorometer with a slit width of 5 nm and excitation and emission wavelengths at 527 nm and 550 nm, respectively, against a standard prepared in the same medium.

In Vitro Release Study of BSA-Loaded Nanoparticles

A known quantity of protein-loaded nanoparticle suspension was centrifuged at 15 000 rpm for 30 minutes at 4°C. The supernatant solution was decanted and the collected nanoparticles were then resuspended and incubated in 5 mL of an aqueous 10 mM phosphate buffer pH 7.4, 100 mM phosphate buffer pH 7.4, or water, each with controlled agitation at 37°C. The quantity of nanoparticles was adjusted to obtain a BSA concentration of 1 mg/mL per release study. At designated time intervals, samples were centrifuged (15 000 rpm) and 5 mL of the supernatant was removed and replaced by an equal volume of fresh medium. The amount of BSA released at various time intervals was determined using the Bradford protein assay method. BSA calibration curves were made with fresh BSA dissolved in the incubation medium. All measurements were performed in triplicate. The empty CS-DS particles were incubated at 37°C and analyzed by the same method to act as controls.

In Vitro Release Study of R6G-Loaded Nanoparticles

A nanoparticle suspension (10 mL with ~2 mg particles) was collected by centrifugation at 15 000 rpm for 15 minutes. After washing in 2.5 mL of water, the nanoparticles were resuspended and incubated in 5 mL of water, 10 mM phosphate buffer pH 7.4, or 10 mM phosphate-buffered saline (PBS; ie, the phosphate buffer containing sodium chloride 0.9% wt/vol) pH 7.4 with controlled agitation at 37°C. At each hour the supernatant samples were isolated by centrifugation at 15 000 rpm for 15 minutes and replaced by an equal volume of fresh medium. The supernatant was analyzed by UV and fluorimetry as described earlier.

Stability of BSA in CS-DS Nanoparticles

The stability of BSA in nanoparticles was investigated by studying the integrity of released BSA by SDS-PAGE analysis. The release samples were lyophilized to concentrate the protein before being used for SDS-PAGE.

The lyophilized release sample was dissolved in 50 μ L Tris-glycine SDS-PAGE sample buffer containing 0.1% bromophenol blue and 20% glycerol. The dissolved sample solutions as well as molecular standards (6.6-200 kDa) were loaded to Tris-glycine gradient gel (8%-16%). The released medium collected from empty CS-DS nanoparticles was treated in the same fashion and used as a control. Gel electrophoresis was performed using a Mini-Protein II cell (Bio-Rad Laboratories) at a constant voltage (150 V) for 90 minutes

Table 1. Effect of Weight Ratio and Charge Ratio of CS:DS on Physicochemical Properties of Empty Nanoparticle Systems*

Weight Ratio of CS:DS	Charge Ratio (N:P)* of the Polymer Mixture	pH of Nanoparticle Dispersion	Conductivity of Dispersion (in millimhos) (SD)	Size (in nm) (SD)	Polydispersity Index (SD)	Zeta Potential (in mV) (SD)
5:3	0.67	3.9	3.83 (0.04)	2110 (398)	0.86 (0.08)	60.0 (1.5)
5:4.5	1.01	4.0	3.72 (0.06)	1894 (187)	0.64 (0.19)	45.2 (1.3)
5:5	1.12	4.0	3.70 (0.10)	345 (11)	0.61 (0.07)	-25.3 (0.8)
5:8.5	1.90	4.0	3.78 (0.04)	244 (8)	0.51 (0.04)	-33.0 (1.6)
5:10	2.24	3.9	3.84 (0.15)	245 (5)	0.48 (0.05)	-40.3 (1.5)
5:20	4.48	4.0	4.52 (0.11)	249 (10)	0.49 (0.03)	-47.1 (0.9)

*Charge ratio (N:P) was calculated based on the number of negatively charged groups (ie, sulfate groups in DS) over that of positively charged groups (ie, protonable amino groups in CS) in the formulation. Both CS and DS solutions were 0.1% wt/vol, and the final volume of the mixture was 40 mL. DS indicates dextran sulfate; CS, chitosan.

using Power PAC 300 (Bio-Rad Laboratories) with a running buffer containing 25 mM Tris, 192 mM glycine, and 0.1% SDS at pH 8.3. The sample bands were stained for 30 minutes with 0.1% Coomassie blue R-250 solution containing 10% acetic acid and 25% isopropanol, followed by destaining overnight with a solution of 50% acetic acid in isopropanol. The separation of BSA on the gel was visualized using a gel image system (Kodak Digital Science 1D, Rochester, NY).

Conductivity Measurement

Conductivity of the nanoparticle dispersion, 0.1% CS, 0.1% DS, and deionized water was determined using a conductivity meter (Systronics 307, Ahmedabad, India) with a conductivity range from 0.1 to 200 millimhos at room temperature. All samples were prepared in deionized water.

RESULTS AND DISCUSSION

Optimization of CS-DS Nanoparticle Formulation

The opposite charges of CS and DS were responsible for the formation of micro- and nanoparticles. The charge ratio between the negatively charged sulfate groups (N) in DS and the positively charged amine groups (P) in CS was calculated for each formulation. Under the experimental conditions (pH 3-4), DS carries ~74 sulfate groups per mole, equivalent to 5.78×10^{-3} negatively charged groups per gram of DS; CS has ~2073 amino groups per mole, equivalent to $\sim 5.18 \times 10^{-3}$ positively charged groups per gram of CS. At the chosen weight ratios of CS:DS, for example 5:3, 5:5, 5:10, and 5:20, the calculated charge ratios in empty micro- and nanoparticles are 0.67, 1.12, 2.24, and 4.48, respectively, as shown in Table 1.

Polymer Concentration

The influence of polymer concentration on particle formation was assessed; the data are presented in Figure 1. Particle sizes obtained from mixing various volumes of 0.1% CS

with 0.1% DS, correlated to different charge ratios, are presented in Table 1. It was observed that nanoparticles of a size less than 500 nm were obtained when 0.1% CS was mixed with 0.1% DS solution at the CS:DS weight ratio 5:5 (N:P 1.12) or below. However, nanosized particles were also obtained with the 5:3 (CS:DS) weight ratio when the final volume of the mixture was low (Table 2). This is possibly due to the increased agitation and/or turbulence created in the small-volume solution.

It was noted that the formation of nanoparticles was strongly influenced by the concentrations of CS and DS. This phenomenon was also observed with CS-TPP nanoparticle preparations.⁵ In general, the formation of small particles was confined to very dilute solutions of CS (initial concentration of 0.1% wt/vol and final concentration less than 0.07%) and DS (initial concentration of 0.1% wt/vol and final concentration less than 0.06%). It is possible that when both polymers were in low concentrations, the addition of DS to the CS resulted in small coacervation nuclei, whereas large coacervates tended to form when polymer concentrations increased to 0.25% wt/vol or above. The mixture of a high concentration

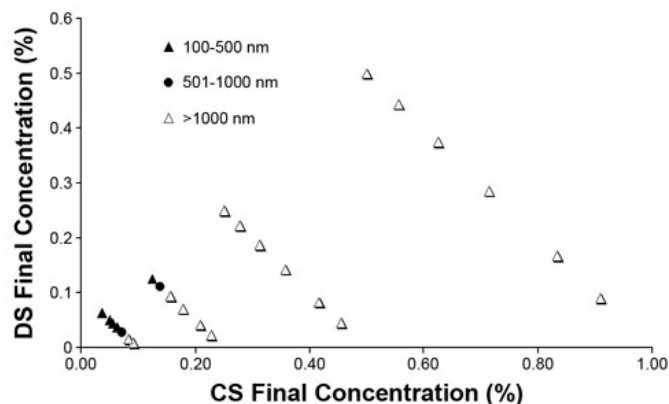


Figure 1. Effect of the final concentrations of matrix materials (CS and DS) on the size of nanoparticles formed. DS indicates dextran sulfate; CS, chitosan.

Table 2. Influence of the CS:DS Weight Ratio and Charge Ratio on Physicochemical Characteristics and BSA Entrapment of Nanoparticles*

Sample	CS:DS Weight Ratio (charge ratio N:P)	pH of Preparation	Conductivity of Dispersion (in Millimhos) (SD)	Size (in nm) (SD)	Polydispersity Index (SD)	Zeta Potential (in mV) (SD)	BSA Loading (%)	Entrapment Efficiency (%)	Yield (%)
Empty	5:3 (0.67)	3.8	3.83 (0.04)	494 (40)	0.68 (0.11)	52.7 (0.9)	—	—	—
Loaded	5:3	3.9	—	1138 (100)	0.97 (0.30)	56.4 (2.4)	29.3	53.2	94.3
Empty	5:5 (1.12)	3.7	3.70 (0.10)	436 (45)	0.70 (0.09)	-23.7 (1.1)	—	—	—
Loaded	5:5	4.0	—	891 (115)	0.75 (0.08)	30.0 (3.2)	33.7	98.9	62.2
Empty	3:5 (1.87)	4.0	3.77 (0.04)	350 (50)	0.55 (0.10)	-32.3 (1.6)	—	—	—
Loaded	3:5	4.0	—	478 (45)	0.64 (0.07)	-28.0 (1.8)	22.7	96.8	94.9
Empty	5:8.5 (1.90)	3.7	3.78 (0.04)	293 (5)	0.58 (0.13)	-32.9 (1.4)	—	—	—
Loaded	5:8.5	3.7	—	660 (20)	0.85 (0.15)	-26.6 (1.2)	24.1	100.0	92.7

*Nanoparticles were prepared from 0.1% CS and 0.1% DS with the final volume of mixture 8 to 13.5 mL. CS indicates chitosan; DS, dextran sulfate; BSA, bovine serum albumin.

of DS with an equally high concentration of CS is more likely to affect the entanglement of the CS chains and solvation in water, leading to the high level of complexation and coacervation. The concentration of 0.1% was identified as optimum for CS and DS, so this concentration was used in all later studies.

Charge Ratio

One of the most important findings of this study is that the charge ratio of N:P determines the properties of CS-DS particles. The charge ratio's effect on particle size overrides that of the method of agitation. For instance, it was observed that at the charge ratio (N:P) of 1.12, homogenization produced nanoparticles of 327 ± 62 nm and magnetic stirring produced particles of 415 ± 74 nm, whereas at the charge ratio of 2.24,

these 2 methods generated nanoparticles of 248 ± 11 nm and 278 ± 9 nm, respectively.

Figure 2a illustrates an interesting trend between the weight ratio or charge ratio (N:P) of CS:DS, particle size, and zeta potential obtained at 0.1% polymer concentrations. An increase in the N:P ratio (ie, more negatively charged polymer DS in the system) correlates with a decrease in particle size and zeta potential. It was postulated that such a trend is caused by the difference in the MW of the 2 oppositely charged ionic polymers. The MW of CS used in this study was 400 kDa, whereas DS's MW was 12.75 kDa. When the final concentration of the long-chain CS molecule in the preparation is high (ie, the charge ratio N:P is low), larger nanoparticles are formed, because the electrostatic repulsion of the CS polymer's ionic groups causes hydration and stretching. On the

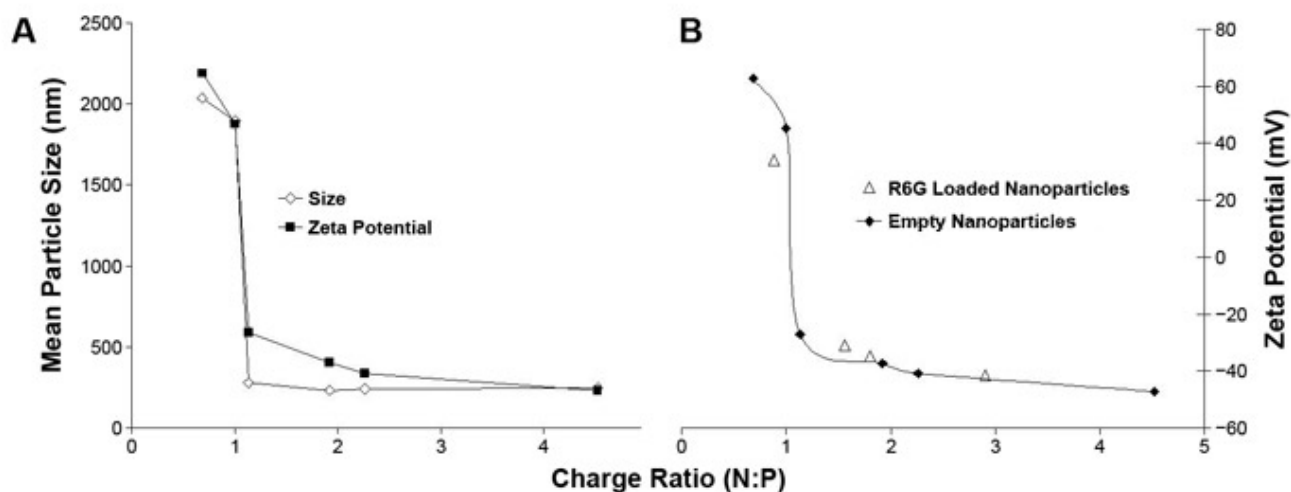


Figure 2. Influence of the charge ratio (a) on the particle size and zeta potential of empty CS-DS particles; and (b) on the zeta potential of empty and R6G-loaded CS-DS particles. R6G indicates rhodamine 6G; CS, chitosan; DS, dextran sulfate.

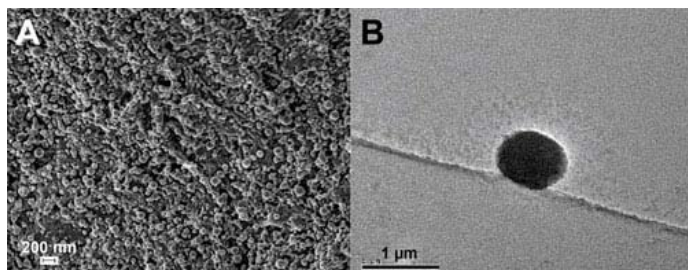


Figure 3. Morphology of CS-DS nanoparticles: (a) field emission scanning electron microscopy image of R6G-loaded CS-DS nanoparticles; (b) transmission electron microscopy image of BSA-loaded CS-DS nanoparticle. CS indicates chitosan; DS, dextran sulfate; R6G, rhodamine 6G; BSA, bovine serum albumin.

other hand, when the final DS concentration increases (ie, the charge ratio N:P is high), the small DS molecule can interpenetrate CS and fill the inter- and intramolecular spaces between the CS molecules to form ionic interactions, neutralizing the positive charge of the CS. As the charge of CS reduces, the CS molecules start to fold, resulting in the formation of condensed particles with a small size. In addition, the excess DS may act as a colloidal protectant via steric hindrance, preventing small particles from coagulating. Consequently, CS-DS nanoparticles also showed much better stability.¹¹

To further examine how the opposite charges of these 2 polymers were responsible for the formation of particle dispersion, the conductivity was determined and correlated to particle size and zeta potential values of the nanoparticle dispersions formed by the mixture of various ratios of CS:DS. The trend in the change in conductivity mirrors the change in the magnitude of the zeta potential. Both showed the lowest value (or magnitude) when the charge ratio N:P was 1:12 or when the weight ratio of CS:DS was 5:5 (Table 1). The conductivity of the nanoparticle dispersion with different CS:DS ratios was 3.83 to 4.52 millimhos, which was between the conductivity of 0.1% CS (3.51 millimhos) and 0.1% DS (4.96 millimhos) but below the algebraic mean of

the 2 conductivity values. This suggests that ionic interaction occurred as soon as CS was mixed with DS solution and that such interaction between the oppositely charged polymers was responsible for the formation of nanoparticles. When protonated amino groups in CS were neutralized by an equivalent amount of sulfate groups as nanoparticles formed, there was less free ionic species in the dispersion, resulting in low conductivity.

Morphology of CS-DS Nanoparticles

Both FESEM and TEM images of CS-DS nanoparticles (Figure 3) show that nanoparticles have a solid and near-consistent structure. Furthermore, the incorporation of BSA into the nanoparticles produced a smooth surface and compact structure. The particle size observed in FESEM is smaller than that measured by the Zetasizer. This is because dried nanoparticles were used in FESEM and TEM, whereas particles in the liquid dispersion were analyzed by the Zetasizer. CS-DS particles are hydrophilic and would be expected to swell in water, thus producing a large hydrodynamic size when measured by the Zetasizer.

Incorporation of R6G and BSA Into CS-DS Nanoparticles

R6G- and BSA-loaded nanoparticles were obtained spontaneously upon the mixing of the DS aqueous solution (0.1% wt/vol) with the CS solution (0.1% wt/vol) under magnetic stirring, with R6G dissolved in DS solution and BSA dissolved in CS solution. The incorporation of either R6G or BSA into the CS-DS nanoparticles resulted in a sharp increase in the particle size and zeta potential of the nanoparticle dispersion (Tables 2 and 3). The same effect of charge ratio on size and zeta potential seen previously with empty CS-DS nanoparticles was observed with R6G- and BSA-loaded particles. That is, the higher charge ratio N:P correlated with smaller particle size. For R6G entrapment, charge ratios of N:P 2.23 and 4.46 produced nanosized particles (Table 3); for BSA, charge ratios of N:P 1.12 or above led to the formation of BSA-loaded nanoparticles (Table 2). It

Table 3. Properties of Empty and R6G-Loaded CS-DS Micro- and Nanoparticles Prepared by Homogenization*

Sample	Weight Ratio of CS:DS	Charge Ratio (N:P)	Size in nm (SD)	Polydispersity Index (SD)	Zeta Potential in mV (SD)	R6G Loading (%)	Entrapment Efficiency (%)	Yield (%)
Empty	5:5	1.12	345 (11)	0.61 (0.07)	-25.3 (0.8)	—	—	—
Loaded	5:5	1.12	3521 (105)	0.68 (0.22)	34.0 (1.2)	18	42	64
Empty	5:10	2.23	245 (5)	0.48 (0.05)	-40.3 (1.5)	—	—	—
Loaded	5:10	2.23	662 (38)	0.58 (0.09)	-31.0 (1.8)	46	98	57
Empty	5:20	4.46	249 (10)	0.49 (0.03)	-47.1 (0.9)	—	—	—
Loaded	5:20	4.46	545 (28)	0.60 (0.11)	-35.0 (1.6)	31	98	69

*R6G indicates rhodamine 6G; CS, chitosan; DS, dextran sulfate.

was observed that when the addition of the drug was likely to cause the neutralization of the particles' net charge, a microsized, rather than nanosized, product was formed. Higher yields were obtained with BSA-loaded nanoparticles than with R6G-loaded particles.

The significant increases in particle size and zeta potential give a good indication of the incorporation of BSA into CS-DS nanoparticles. As the isoelectric point of BSA is 4.8, the BSA would be positively charged at the pH of the formulation medium (3.5-4.0, which was used to maximize the solubility of CS). Hence, positively charged BSA could compete with CS to interact with DS electrostatically. This ionic interaction, provided by the multi-ionic sites of the large-molecule BSA, may have contributed to the strong association of BSA with the nanoparticles, indicated by the high entrapment efficiency and the increase of the nanoparticles' positive charge (Table 2).

A study was undertaken to investigate the effect of the order of BSA mixing with CS and DS. The data obtained show that the order of BSA mixing had no effect on the size, entrapment efficiency, and yield of BSA-loaded nanoparticles. Hence, for all other work, BSA-loaded nanoparticles were prepared using BSA dissolved in CS solution.

The BSA entrapment efficiency was found to be affected by the charge ratio: the higher the charge ratio N:P, the higher the entrapment efficiency. The maximum efficiency of 100% was achieved with the charge ratio of 1.90 and weight ratio CS:DS of 5:8.5. Protein association studies performed by Calvo et al at different pH values¹⁶ indicated that there was a significant incorporation of BSA into CS/TPP nanoparticles at all pH values but the greatest loading efficiency was obtained when the protein was dissolved at a pH above its isoelectric point (ie, when BSA was predominantly negatively charged and therefore could ionically interact with CS). Lim's group reported that the formulation pH modulates the interaction of insulin with CS/TPP nanoparticles in a similar fashion, with the maximum association efficiency of insulin achieved at pH 6.1 when insulin is negatively charged.¹⁴ This suggests that the major factor that leads to the association of protein to the CS nanoparticle might be the protein-polysaccharide electrostatic interaction, although other mechanisms such as reduction of protein solubility near its isoelectric point, hydrogen bonding, and hydrophobic interactions might also be involved. The observation that the incorporation efficiency increased with the DS ratio and the magnitude of the negative charge of the nanoparticles strongly supports the hypothesis that ionic interaction is the major factor contributing to the incorporation of BSA into CS-DS nanoparticles. Unlike other reports in which maximum protein association with CS nanoparticles could be achieved only when the protein was negatively charged, the formulation described in this study allows the maximum

incorporation of protein when it is positively charged. This has important implications for the nanoparticle formulation of positively charged proteins and peptides.

The formulation of nanoparticles at a pH near the isoelectric point of the protein may reduce the solubility of the protein and increase the apparent protein entrapment in nanoparticles. However, being zwitterionic, protein molecules tend to undergo hydrophobic self-association or hydrophobic interactions and H-bonding with CS. Such association or interaction with CS, however, is much weaker compared with ionic interaction, and the equilibrium could rapidly shift toward dissociation with small pH changes or by dilution, resulting in fast release, as reported with insulin.¹⁴

Like entrapment of BSA, entrapment of R6G in CS-DS nanoparticles resulted in enlarged particle size and elevated zeta potential compared with empty particles (Table 3). To produce nanosized R6G-loaded particles, the charge ratio of N:P had to be 2.24 or greater. Such a high charge ratio increased the entrapment efficiency markedly, to 98%, indicating that almost all R6G was incorporated into the CS-DS nanoparticles via ionic interaction. This was further supported by the observation that the relationship between the charged groups and the zeta potential of nanoparticles was predictable and could be established and used as a calibration curve (produced by using empty nanoparticles) to estimate the zeta potential of a CS-DS nanoparticle system containing a small ionic drug such as R6G. The measured zeta potential of the nanoparticles loaded with a known amount of R6G showed a good correlation with the theoretical value calculated by the calibration curve (Figure 2b), with a correlation coefficient of 0.9992 (the positive charges contributed by R6G were taken into account). Hence, it could be concluded that the ionic interaction between the sulfate groups (N) in DS and amino and imine groups (P) in R6G determines R6G entrapment. The latter can be estimated by the relationship between the charge ratio or charge groups and the zeta potential.

In Vitro Release Studies

The release profiles of R6G- and BSA-loaded nanoparticles were evaluated in water and a phosphate buffer, which was either in a different ionic strength or with saline, to study the underpinning mechanisms for drug release. The greatest release for both R6G- and BSA-loaded nanoparticles occurred in the release media of a high ionic strength (PBS and a 100 mM phosphate buffer, respectively). In contrast, a significantly small portion of R6G and BSA was released in water over the release study period (Figures 4 and 5). The burst release was observed with both types of nanoparticles, and it may have arisen from the desorption of loosely attached R6G and BSA from the surface of the matrix polymers.

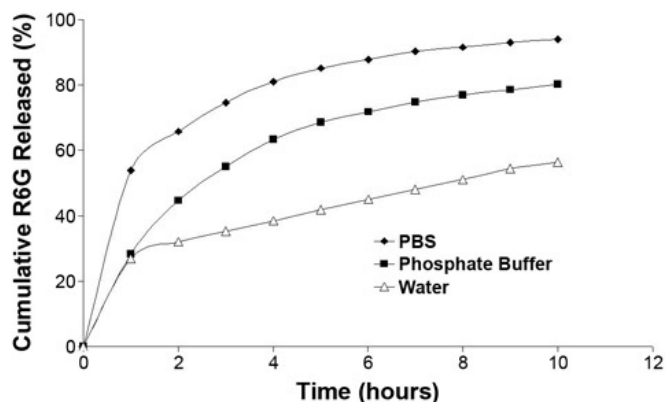


Figure 4. Cumulative release of R6G from nanoparticles prepared using CS:DS weight ratio of 5:5 (charge ratio N:P 1.12) in different release media. R6G indicates rhodamine 6G; PBS, phosphate-buffered saline; CS, chitosan; DS, dextran sulfate.

There was a vast difference in release profiles between R6G and BSA. R6G displayed a constant release rate in water after initial burst release, possibly through dissociation/diffusion (Figure 4), whereas BSA showed almost no release in water after the first 2 time points (Figure 5). The huge difference in the release pattern was also shown in other release media (medium and high ionic strength of buffers with the same pH). For instance, close to 80% and 100% of the loaded R6G was released in the 10 mM phosphate buffer and PBS after 10 hours, whereas only ~30% and 65% of the loaded BSA was released in the 10 and 100 mM phosphate buffer over a period of 7 days. Such differences could be caused by the large molecule size of BSA, rendering difficulties in total dissociation via ion exchange and diffusion through the CS-DS matrix structure. It is evident that both the molecular size of the drug and ion exchange (or ionic interaction), rather than the pH difference between water

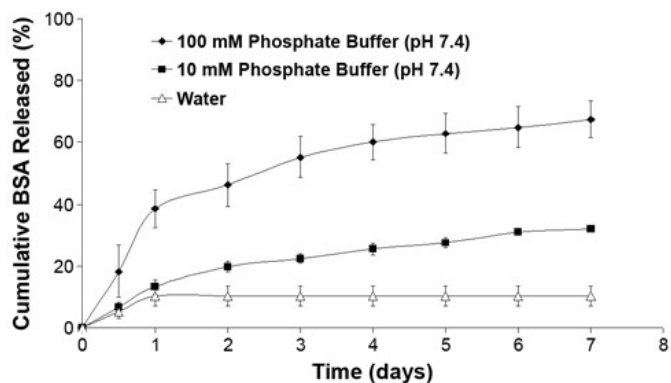


Figure 5. Cumulative release of BSA from nanoparticles prepared using CS:DS weight ratio of 5:8.5 (charge ratio N:P 1.90) in different release media. BSA indicates bovine serum albumin; CS, chitosan; DS, dextran sulfate.

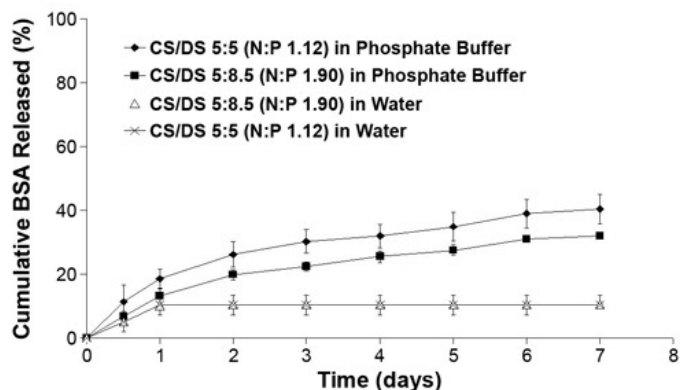


Figure 6. Cumulative release of BSA from nanoparticles with different CS:DS weight ratios and charge ratios in 10 mM phosphate buffer (pH 7.4) and water. BSA indicates bovine serum albumin; CS, chitosan; DS, dextran sulfate.

and the pH 7.4 phosphate buffer, affect the rate of the BSA and R6G release.

The results of the effect of charge ratio on BSA release from nanoparticles are presented in Figure 6. The data show that an increase of the charge ratio from 1.12 to 1.90 in the nanoparticle formulation resulted in a reduction of burst release, contributing to less BSA release in phosphate buffer. However, such an increase in the charge ratio did not result in a change in BSA release in water with both nanoparticles showed very similar release profiles in water.

Calvo et al^{5,16} observed that the percentage in vitro release of BSA from CS-TPP nanoparticles was greater for those formulations containing higher protein loading; the finding here is consistent with their observation. In this study the BSA loading capacity of 5:8.5 ratio (charge ratio N:P 1.90) CS-DS nanoparticles was 24.1% wt/wt, compared with the 33.7% wt/wt of 5:5 ratio (charge ratio N:P 1.12) nanoparticles. The release rate of 5:5 ratio CS-DS nanoparticles was faster than that of the 5:8.5 ratio in 10 mM phosphate buffer pH 7.4. However, the higher proportion of DS in nanoparticles may have resulted in a larger proportion of positively charged BSA being bound to the negative DS in 5:8.5 CS-DS nanoparticles via ionic interaction and therefore a slower BSA release.

Stability of BSA in CS-DS Nanoparticles

When nanoparticles are used for protein delivery, the protein must be protected by the nanoparticle formulation during its production, storage, and application. The stability and integrity of BSA in nanoparticles were evaluated by gel electrophoresis. Figure 7 shows the SDS-PAGE analysis of release fractions of BSA, BSA standards, and empty nanoparticles that were used as a control. The gel electrophoresis study on BSA that had endured the loading and release process at

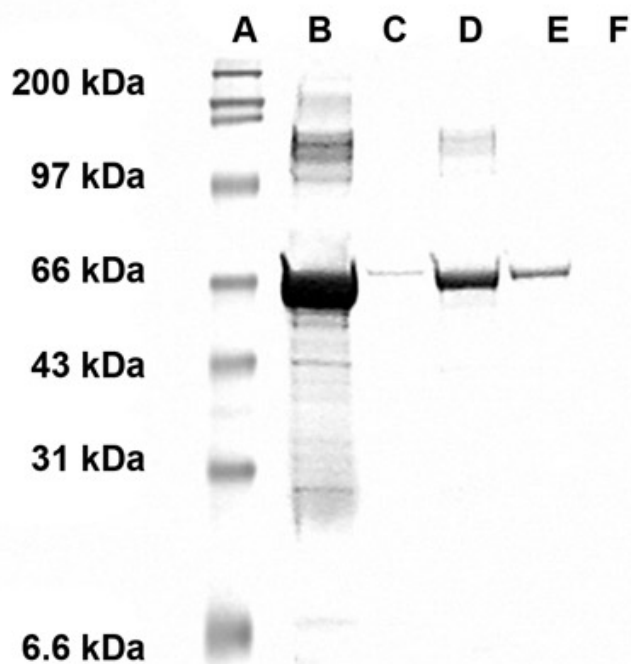


Figure 7. Sodium dodecyl sulfate–polyacrylamide gel electrophoresis analysis of stability of BSA released from CS-DS nanoparticles: (A) molecular weight; (B) and (C) BSA standards, 0.5 and 0.02 mg/mL; (D) and (E) BSA released on day 1 and day 5; (F) empty particle control on day 5. BSA indicates bovine serum albumin; CS, chitosan; DS, dextran sulfate.

37°C confirmed that the integrity of BSA released on day 1 or 5 is no different from that of freshly prepared BSA standards. It can be concluded that BSA remained in its native form in the CS-DS nanoparticles under the experimental conditions described here.

Recently, Peng et al showed that adding different anions and controlling their concentrations did not influence DNA encapsulation in CS nanoparticles but did reduce CS nanoparticles' nonspecific interaction with cell membranes and therefore their toxicity.¹⁷ Although the potential toxicity of CS-DS is yet to be determined, it is postulated that the toxicity of CS-DS nanoparticles could be lower than that of positively charged CS nanoparticles because of the reduction in nonspecific interaction with cell membranes as a result of the decrease in cationic charge of the nanoparticles.

CONCLUSION

This study has demonstrated that modulation of the charge ratio of N:P can permit control of particle size, surface charge, level of R6G and BSA loading, and R6G and BSA release. Ionic interaction is the major mechanism controlling both the incorporation of ionizable drugs and their release from CS-DS nanoparticles. This study has significant implications for the application of CS-DS nanoparticles for de-

livery of positively or negatively charged and amphoteric molecules. The convenient formulation and production, and the ability to maintain protein activity, render CS-DS nanoparticles a promising drug delivery system for the parenteral and mucosal administration of biomolecules such as peptides, proteins, and gene materials.

REFERENCES

1. Agnihotri SA, Mallikarjuna NN, Aminabhavi TM. Recent advances on chitosan-based micro- and nanoparticles in drug delivery. *J Control Release*. 2004;100:5–28.
2. Illum L, Jabbar-Gill I, Hinchcliffe M, Fisher AN, Davis SS. Chitosan as a novel nasal delivery system for vaccines. *Adv Drug Deliv Rev*. 2001;51:81–96.
3. Tang ESK, Huang M, Lim LY. Ultrasonication of chitosan and chitosan nanoparticles. *Int J Pharm*. 2003;265:103–114.
4. Sinha VR, Singla AK, Wadhawan S, et al. Chitosan microspheres as a potential carrier for drugs. *Int J Pharm*. 2004;274:1–33.
5. Calvo P, Remunan-Lopez C, Vila-Jato JL, Alonso MJ. Novel hydrophilic chitosan-polyethylene oxide nanoparticles as protein carriers. *J Appl Polym Sci*. 1997;63:125–132.
6. De S, Robinson D. Polymer relationships during preparation of chitosan-alginate and poly-L-lysine-alginate nanospheres. *J Control Release*. 2003;89:101–112.
7. Fernandez-Urrusuno R, Calvo P, Remunan-Lopez C, Vila-Jato JL, Alonso MJ. Enhancement of nasal absorption of insulin using chitosan nanoparticles. *Pharm Res*. 1999;16:1576–1581.
8. Xu Y, Du Y. Effect of molecular structure of chitosan on protein delivery properties of chitosan nanoparticles. *Int J Pharm*. 2003; 250:215–226.
9. Chen Y, Mohanraj V, Parkin J. Chitosan-dextran sulfate nanoparticles for delivery of an anti-angiogenesis peptide. *Int J Pept Res Ther*. 2003; 10:621–629.
10. Pan Y, Li Y-j, Zhao H-y, et al. Bioadhesive polysaccharide in protein delivery system: chitosan nanoparticles improve the intestinal absorption of insulin in vivo. *Int J Pharm*. 2002;249:139–147.
11. Wang F. *Micro and Nanoparticles for Site-Specific Drug Delivery in the Skin [master's thesis]*. [thesis]. Perth, Australia: School of Pharmacy, Curtin University of Technology; 2005.
12. Tiyaboonchai W, Woiszwillo J, Middaugh CR. Formulation and characterization of DNA-polyethylenimine-dextran sulfate nanoparticles. *Eur J Pharm Sci*. 2003;19:191–202.
13. Tiyaboonchai W, Woiszwillo J, Sims RC, Middaugh CR. Insulin containing polyethylenimine-dextran sulfate nanoparticles. *Int J Pharm*. 2003;255:139–151.
14. Ma Z, Yeoh HH, Lim LY. Formulation pH modulates the interaction of insulin with chitosan nanoparticles. *J Pharm Sci*. 2002;91:1396–1404.
15. Bradford M. A rapid and sensitive method for the quantitation of microgram quantities of protein utilizing the principle of protein-dye binding. *Anal Biochem*. 1976;72:248–254.
16. Calvo P, Remunan-Lopez C, Vila-Jato JL, Alonso MJ. Chitosan and chitosan/ethylene oxide-propylene oxide block copolymer nanoparticles as novel carriers for proteins and vaccines. *Pharm Res*. 1997;14:1431–1436.
17. Peng J, Xing X, Wang K, Tan W, He X, Huang S. Influence of anions on the formation and properties of chitosan-DNA nanoparticles. *J Nanosci Nanotechnol*. 2005;5:713–717.